Journée GT6 Mécanismes Reconfigurables 2016
Clermont Ferrand

Comparison of some Zero-torsion Parallel Manipulators based on their Maximum Inscribed Singularity-free Circle and Parasitic motion

Abhilash NAYAK, Latifah NURAHMI,
Philippe WENGER, Stéphane CARO

IRCCyN, Ecole Centrale de Nantes

3 October 2016

Applications of zero-torsion PMs

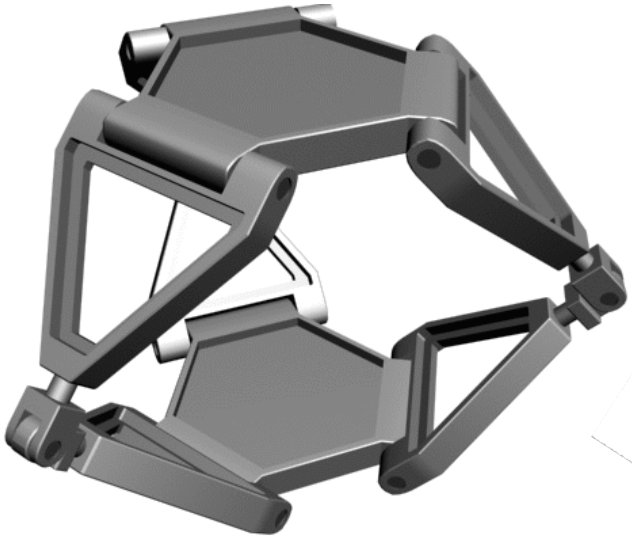

Canfield's joint (3-RSR)
Canfield et al. 1996

Z3 sprint (3-PRS)
Wahl, 2006

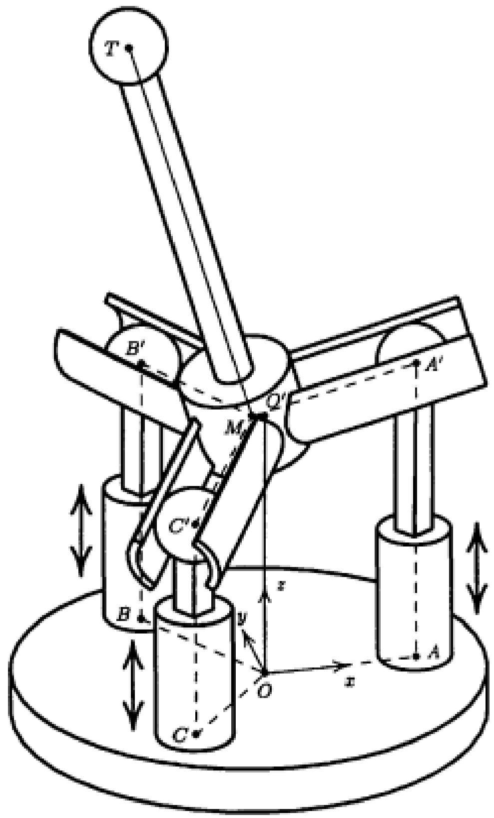

Robotic finger (3-PSP)
Tischler et al., 1998

Zero-torsion mechanisms

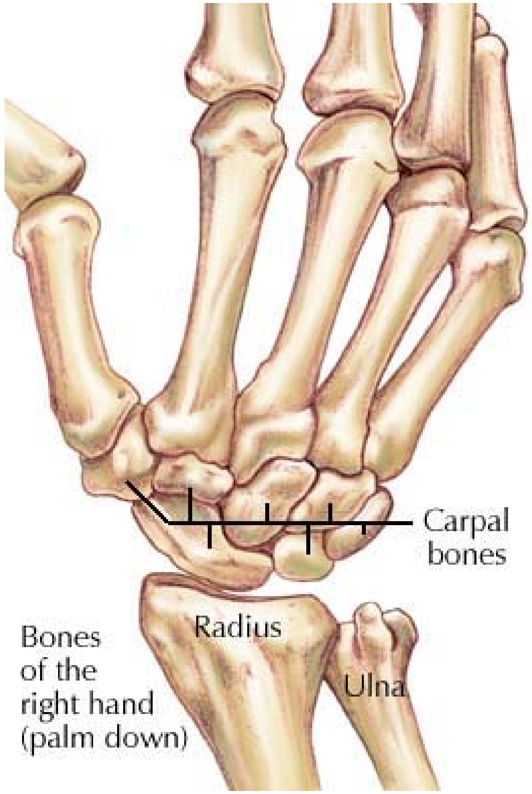

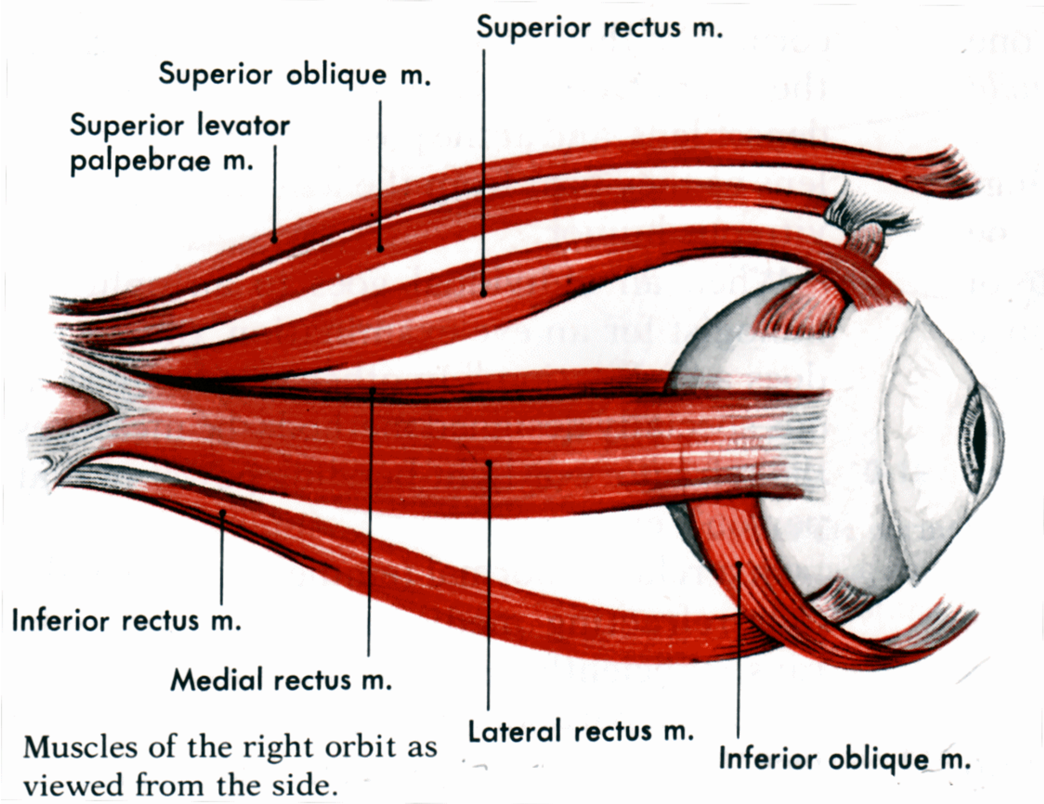

Courtesy : Wikipedia

Contents

1 Manipulator Architecture

3-RPS parallel manipulator [1]

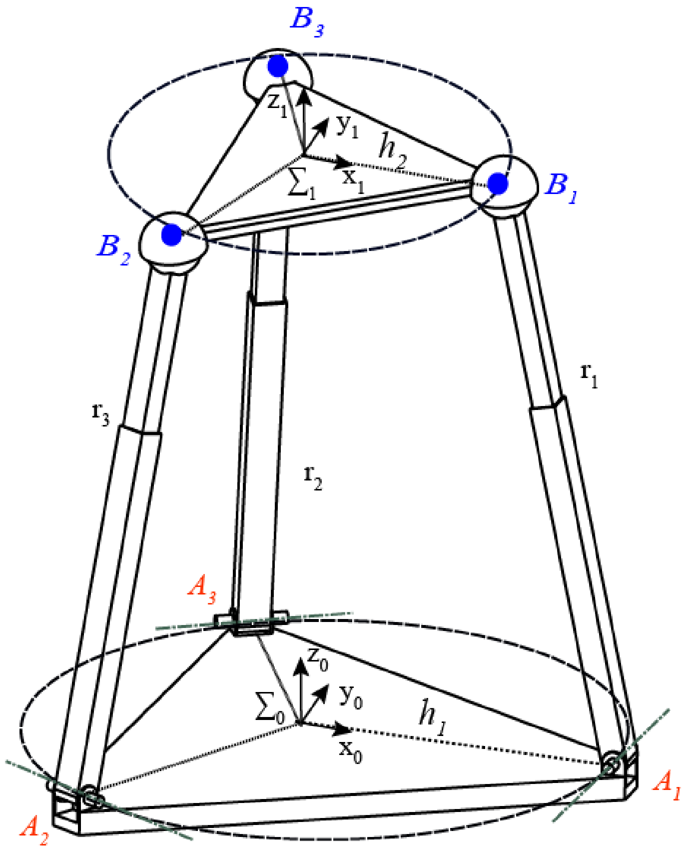

3-SPR parallel manipulator

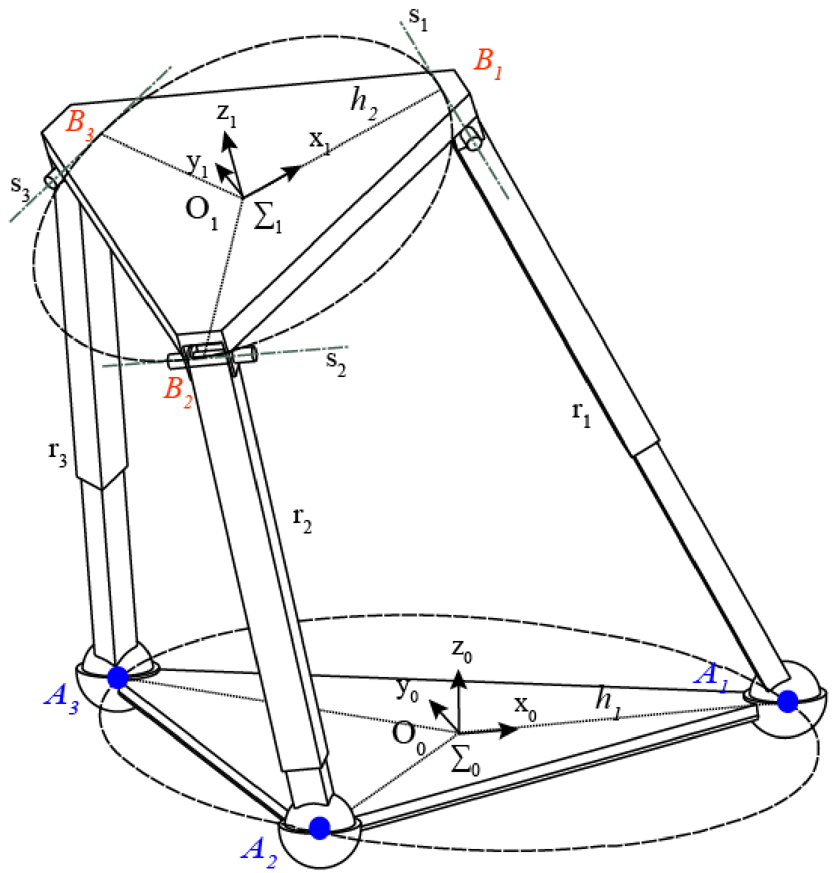

[1] Schadlbauer, J., Walter, D.R., and Husty, M.: A Complete Kinematic Analysis of the 3-RPS Parallel Manipulator, 15th National Conference on Machines and Mechanisms (2011).

1 Manipulator Architecture

3-PRS parallel manipulator [2]

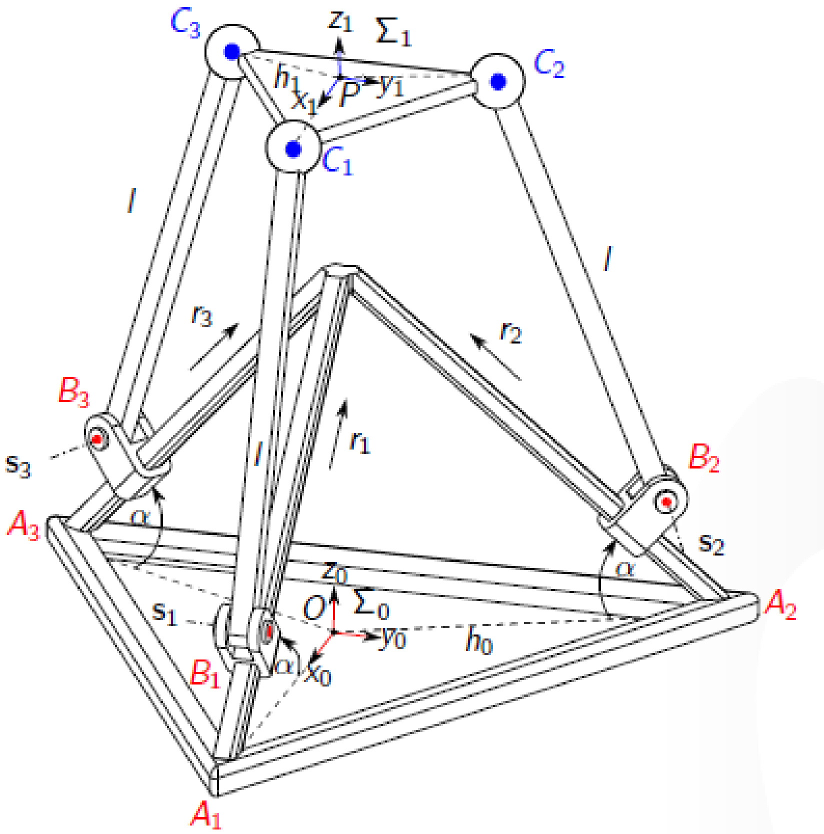

3-PUU parallel manipulator [3]

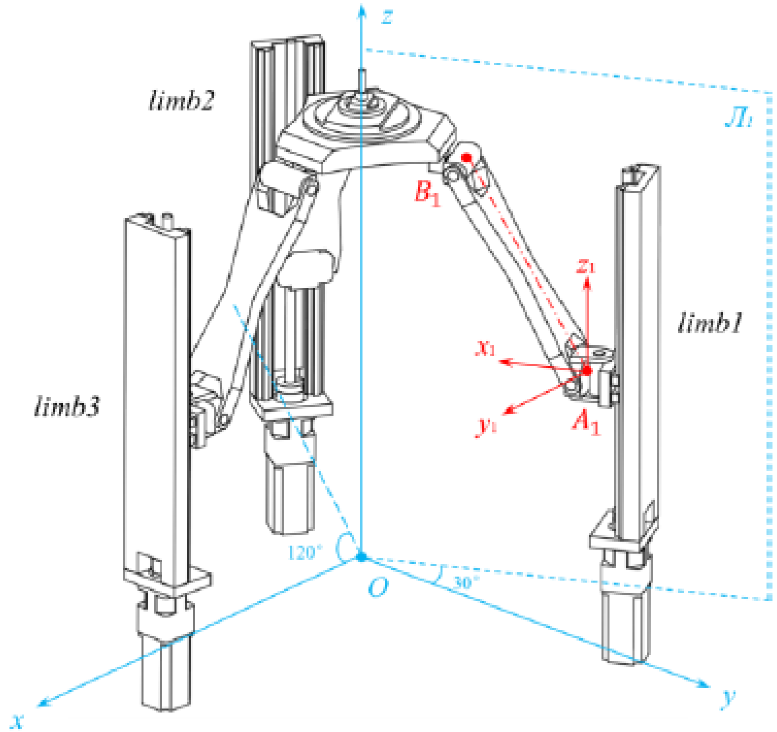

[2] Latifah Nurahmi et al. Operation Modes and Singularities of 3-PRS Parallel Manipulators With Different Arrangements of P-Joints

[3] Wang Liping et al. Optimal design of a 3-PUU parallel mechanism with 2R1T DOFs

1 Manipulator Architecture

3-SPR parallel manipulator

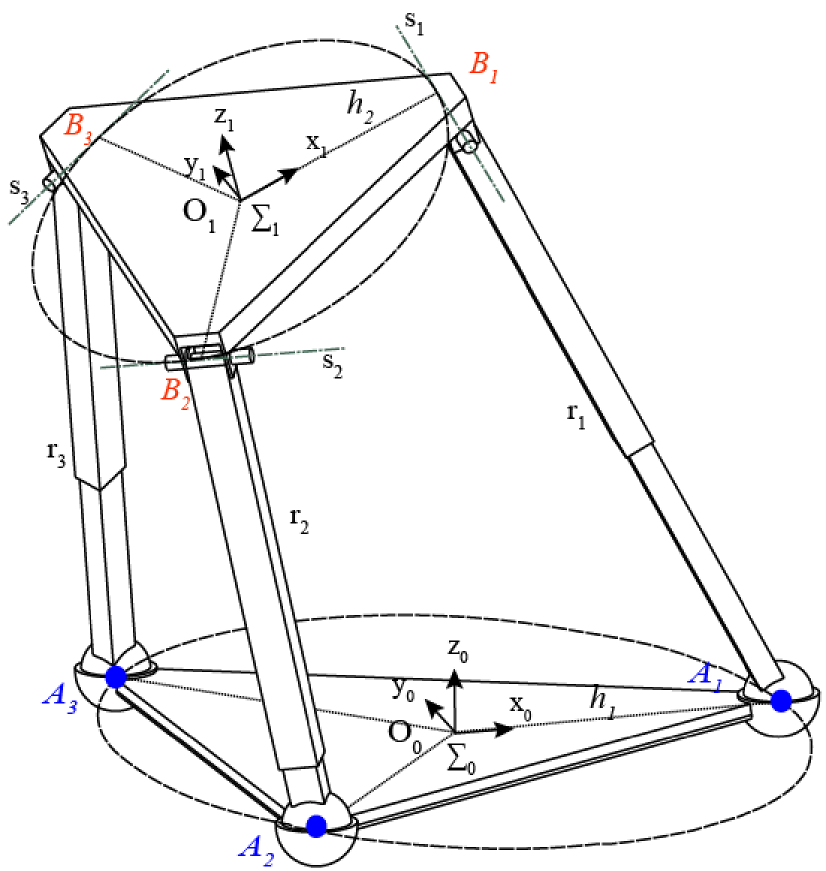

$$\mathbf{r}_{A_1}^0 = [1, h_1, 0, 0]^T$$

$$\mathbf{r}_{A_2}^0 = [1, -\frac{1}{2}h_1, -\frac{\sqrt{3}}{2}h_1, 0]^T$$

$$\mathbf{r}_{A_3}^0 = [1, -\frac{1}{2}h_1, \frac{\sqrt{3}}{2}h_1, 0]^T$$

$$\mathbf{r}_{B_1}^1 = [1, h_2, 0, 0]^T$$

$$\mathbf{r}_{B_2}^1 = [1, -\frac{1}{2}h_2, -\frac{\sqrt{3}}{2}h_2, 0]^T$$

$$\mathbf{r}_{B_3}^1 = [1, -\frac{1}{2}h_2, \frac{\sqrt{3}}{2}h_2, 0]^T$$

2 Constraint equations : 3-S<u>P</u>R parallel manipulator

Study's kinematic mapping [1]

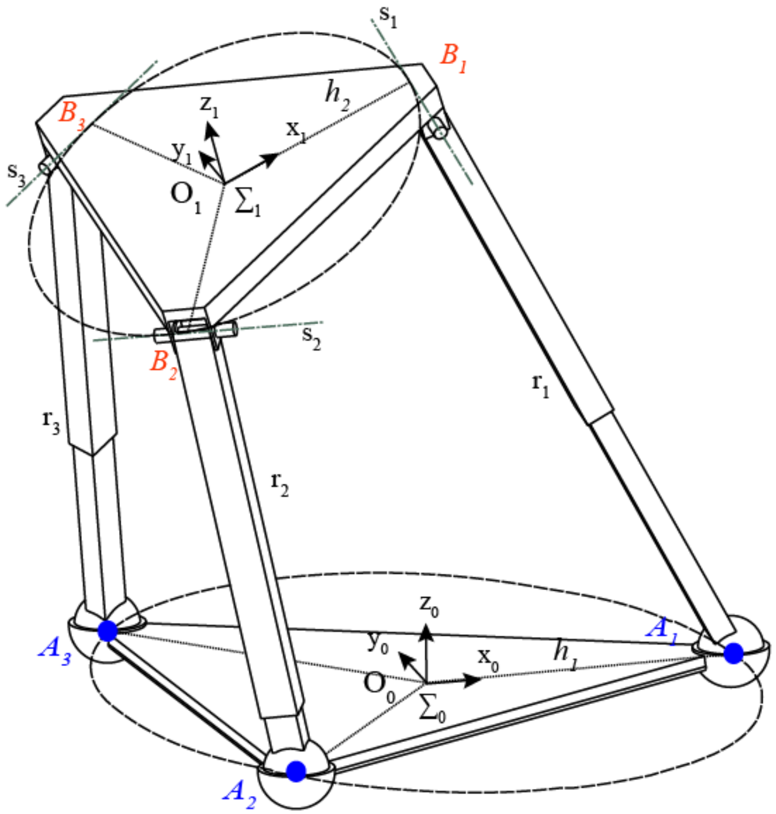

$$\gamma : \mathbb{R}^3 \rightarrow \mathbb{R}^3,\ \ \mathbf{x} = \mathbf{A}\mathbf{x} + \mathbf{d} \quad \longrightarrow \quad p \in \mathbb{P}^7$$

$$\mathbf{M} = \begin{bmatrix} x_0{}^2 + x_1{}^2 + x_2{}^2 + x_3{}^2 & \mathbf{0}_{3\times 1}^T \\ \mathbf{M}_T & \mathbf{M}_R \end{bmatrix}$$

$$\mathbf{M}_T = \begin{bmatrix} -2x_0y_1 + 2x_1y_0 - 2x_2y_3 + 2x_3y_2 \\ -2x_0y_2 + 2x_1y_3 + 2x_2y_0 - 2x_3y_1 \\ -2x_0y_3 - 2x_1y_2 + 2x_2y_1 + 2x_3y_0 \end{bmatrix}$$

$$\mathbf{M}_R = \begin{bmatrix} x_0{}^2 + x_1{}^2 - x_2{}^2 - x_3{}^2 & -2x_0x_3 + 2x_1x_2 & 2x_0x_2 + 2x_1x_3 \\ 2x_0x_3 + 2x_1x_2 & x_0{}^2 - x_1{}^2 + x_2{}^2 - x_3{}^2 & -2x_0x_1 + 2x_3x_2 \\ -2x_0x_2 + 2x_1x_3 & 2x_0x_1 + 2x_3x_2 & x_0{}^2 - x_1{}^2 - x_2{}^2 + x_3{}^2 \end{bmatrix}$$

[1] Schadlbauer, J., Walter, D.R., and Husty, M.: A Complete Kinematic Analysis of the 3-RPS Parallel Manipulator, 15th National Conference on Machines and Mechanisms (2011).

2 Constraint equations : 3-S<u>P</u>R parallel manipulator

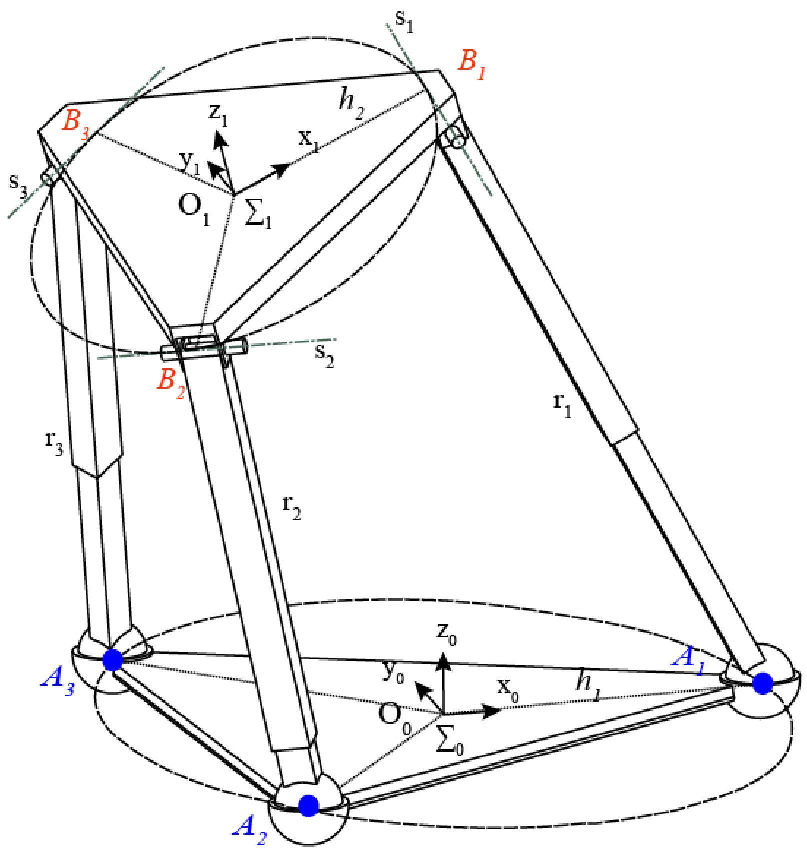

$$\mathbf{r}_{B_i}^0 = \mathbf{M}\,\mathbf{r}_{B_i}^1 \qquad \mathbf{s}_i^0 = \mathbf{M}\,\mathbf{s}_i^1 \qquad i = 1, 2, 3$$

Plane constraint equations

$$(\mathbf{r}_{B_i}^0 - \mathbf{r}_{A_i}^0)^T \mathbf{s}_i = 0$$

$$g_1 := x_0 x_3 = 0$$

$$g_2 := h_1 {x_1}^2 - h_1 {x_2}^2 - 2\,x_0 y_1 + 2\,x_1 y_0 + 2\,x_2 - 2\,x_3 y_2 = 0$$

$$g_3 := 2\,h_1 x_0 x_3 + h_1 x_1 x_2 + x_0 y_2 + x_1 y_3 - x_2 y_0 - x_3 y_1 = 0$$

2 Constraint equations : A comparison

3-S<u>P</u>R parallel manipulator $(x_0, -x_1, -x_2, -x_3, y_0, -y_1, -y_2, -y_3)$

$$
\begin{aligned}
g_1 &:= x_0 x_3 = 0 \\
g_2 &:= h_1 {x_1}^2 - h_1 {x_2}^2 - 2x_0 y_1 + 2x_1 y_0 + 2x_2 y_3 - 2x_3 y_2 = 0 \\
g_3 &:= 2h_1 x_0 x_3 + h_1 x_1 x_2 + x_0 y_2 + x_1 y_3 - x_2 y_0 - x_3 y_1 = 0
\end{aligned}
$$

3-R<u>P</u>S parallel manipulator $(x_0, x_1, x_2, x_3, y_0, y_1, y_2, y_3)$

$$
\begin{aligned}
g_1 &:= x_0 x_3 = 0 \\
g_2 &:= h_1 {x_1}^2 - h_1 {x_2}^2 + 2x_0 y_1 - 2x_1 y_0 + 2x_2 y_3 - 2x_3 y_2 = 0 \\
g_3 &:= -2h_1 x_0 x_3 + h_1 x_1 x_2 - x_0 y_2 + x_1 y_3 + x_2 y_0 - x_3 y_1 = 0
\end{aligned}
$$

3-<u>P</u>RS parallel manipulator $(x_0, x_1, x_2, x_3, y_0, y_1, y_2, y_3)$

$$
\begin{aligned}
g_1 &:= x_0 x_3 = 0 \\
g_2 &:= h_1 {x_1}^2 - h_1 {x_2}^2 + 2x_0 y_1 - 2x_1 y_0 + 2x_2 y_3 - 2x_3 y_2 = 0 \\
g_3 &:= -2h_1 x_0 x_3 + h_1 x_1 x_2 - x_0 y_2 + x_1 y_3 + x_2 y_0 - x_3 y_1 = 0
\end{aligned}
$$

3-<u>P</u>UU parallel manipulator $(x_0, x_1, x_2, x_3, y_0, y_1, y_2, y_3)$

$$
\begin{aligned}
g_1 &:= x_0 x_3 = 0 \\
g_2 &:= h_2 {x_1}^2 - h_2 {x_2}^2 - 2x_0 y_1 + 2x_1 y_0 + 2x_2 y3 - 2x_3 y_2 = 0 \\
g_3 &:= 2h_2 x_0 x_3 + h_2 x_1 x_2 + x_0 y_2 + x_1 y_3 - x_2 y_0 - x_3 y_1 = 0
\end{aligned}
$$

2 Constraint equations : 3-S<u>P</u>R parallel manipulator

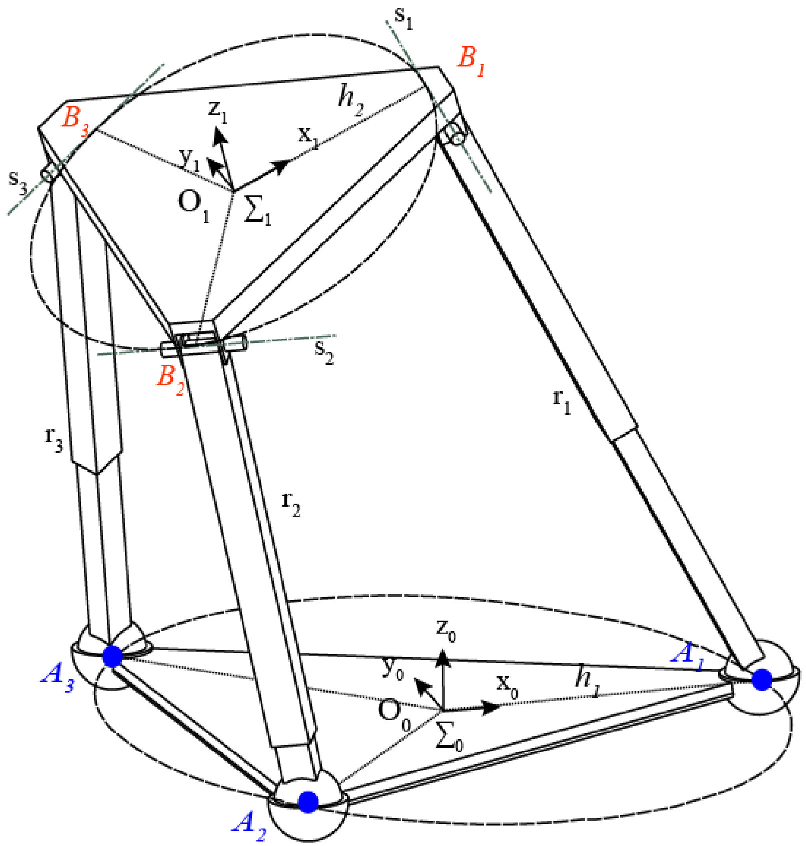

Sphere constraint equations

$$||\mathbf{r}^0_{B_i} - \mathbf{r}^0_{A_i}||^2 = r_i^2$$

Study equation ; Normalization equation

$$g_7 := x_0y_0 + x_1y_1 + x_2y_2 + x_3y_3 = 0$$

$$g_8 := {x_0}^2 + {x_1}^2 + {x_2}^2 + {x_3}^2 - 1 = 0$$

Operation modes

$$\mathcal{I} = < g_1, g_2, g_3, g_4, g_5, g_6, g_7, g_8 >$$

Variables

$\{x_0, x_1, x_2, x_3, y_0, y_1, y_2, y_3\}$

Ring

$\mathbb{C}[h_1, h_2, r_1, r_2, r_3]$

3 Operation modes : 3-S$\underline{\text{P}}$R parallel manipulator

Primary decomposition (singular)

$$\mathcal{J} =< g_1, g_2, g_3, g_7 >$$

$$g_1 := x_0x_3 = 0$$
$$g_2 := h_1{x_1}^2 - h_1{x_2}^2 - 2\,x_0y_1 + 2\,x_1y_0 + 2\,x_2 - 2\,x_3y_2 = 0$$
$$g_3 := 2\,h_1x_0x_3 + h_1x_1x_2 + x_0y_2 + x_1y_3 - x_2y_0 - x_3y_1 = 0$$
$$g_7 := x_0y_0 + x_1y_1 + x_2y_2 + x_3y_3 = 0$$

$$\begin{aligned}\mathcal{J}_1 : \langle & x_0, x_1y_1 + x_2y_2 + x_3y_3, h_1x_1x_2 + x_1y_3 - x_2y_0 - x_3y_1, h_1{x_1}^2 - h_1{x_2}^2 \\ & + 2\,x_1y_0 + 2\,x_2y_3 - 2\,x_3y_2, h_1{x_2}^2y_2 + h_1x_2x_3y_3 - x_1y_1y_3 + x_2y_0y_1 \\ & + x_3{y_1}^2, h_1{x_2}^3 + {x_1}^2y_3 - 3\,x_1x_2y_0 - x_1x_3y_1 - 2\,{x_2}^2y_3 + 2\,x_2x_3y_2, \\ & h_1x_1x_2y_2 + h_1x_1x_3y_3 + h_1{x_2}^2y_1 - 2\,x_1y_0y_1 - 2\,x_2y_1y_3 + 2\,x_3y_1y_2, \\ & {h_1}^2{x_2}^2y_3 - h_1x_1y_0y_3 + h_1x_2{y_1}^2 - 3\,h_1x_2{y_2}^2 - h_1x_2{y_3}^2 - h_1x_3y_2y_3 \\ & - 2\,{y_0}^2y_3 - 2\,{y_1}^2y_3 - 2\,{y_2}^2y_3 - 2\,{y_3}^3, -{h_1}^2{x_2}^2y_0y_3 + {h_1}^2{x_2}^2y_1y_2 \\ & + {h_1}^2x_2x_3y_1y_3 + h_1x_1{y_0}^2y_3 - h_1x_1{y_1}^2y_3 + 3\,h_1x_2y_0{y_2}^2 + h_1x_2y_0{y_3}^2 \\ & + h_1x_3y_0y_2y_3 + h_1x_3{y_1}^3 + 2\,{y_0}^3y_3 + 2\,y_0{y_1}^2y_3 + 2\,y_0{y_2}^2y_3 + 2\,y_0{y_3}^3 \rangle\end{aligned}$$

$$\begin{aligned}\mathcal{J}_2 : \langle & x_3, x_0y_0 + x_1y_1 + x_2y_2, h_1x_1x_2 + x_0y_2 + x_1y_3 - x_2y_0, h_1{x_1}^2 \\ & - h_1{x_2}^2 - 2\,x_0y_1 + 2\,x_1y_0 + 2\,x_2y_3, h_1{x_2}^3 + x_0x_1y_2 + 2\,x_0x_2y_1 \\ & + {x_1}^2y_3 - 3\,x_1x_2y_0 - 2\,{x_2}^2y_3, {h_1}^2{x_2}^2y_0 - h_1x_1{y_0}^2 - h_1x_1{y_2}^2 \\ & - h_1x_2y_0y_3 - 3\,h_1x_2y_1y_2 - 2\,{y_0}^3 - 2\,y_0{y_1}^2 - 2\,y_0{y_2}^2 - 2\,y_0{y_3}^2 \rangle\end{aligned}$$

$$\mathcal{J}_3 : \langle x_0, x_1, x_2, x_3 \rangle$$

3 Operation modes : 3-S<u>P</u>R parallel manipulator

Operation mode 1 : $\mathcal{K}_1$

$$\boxed{x_0 = 0}$$

180^0 displacement of the moving platform w.r.t the fixed base about the ISA[4]

$$cos(\frac{\phi}{2}) = x_0 \quad ; \quad s = \frac{2y_0}{\sqrt{x_1^2 + x_2^2 + x_3^2}}$$

Operation mode 2 : $\mathcal{K}_2$.

$$\boxed{x_3 = 0}$$

ISA is always parallel to the x_0y_0-plane[4]

$$\begin{aligned} p_{01} &= (-x_1^2 - x_2^2 - x_3^2)x_1, & p_{23} &= x_0y_0x_1 - (-x_1^2 - x_2^2 - x_3^2)y_1 \\ p_{02} &= (-x_1^2 - x_2^2 - x_3^2)x_2, & p_{31} &= x_0y_0x_2 - (-x_1^2 - x_2^2 - x_3^2)y_2 \\ p_{03} &= (-x_1^2 - x_2^2 - x_3^2)x_3, & p_{12} &= x_0y_0x_3 - (-x_1^2 - x_2^2 - x_3^2)y_3 \end{aligned}$$

[4] Kong, X.: Reconfiguration analysis of a 3-DOF parallel mechanism using Euler parameter quaternions and algebraic geometry method, Mechanism and Machine Theory, 75, pp. 188-201 (2014).

3 Operation modes : 3-S$\underline{\text{P}}$R parallel manipulator

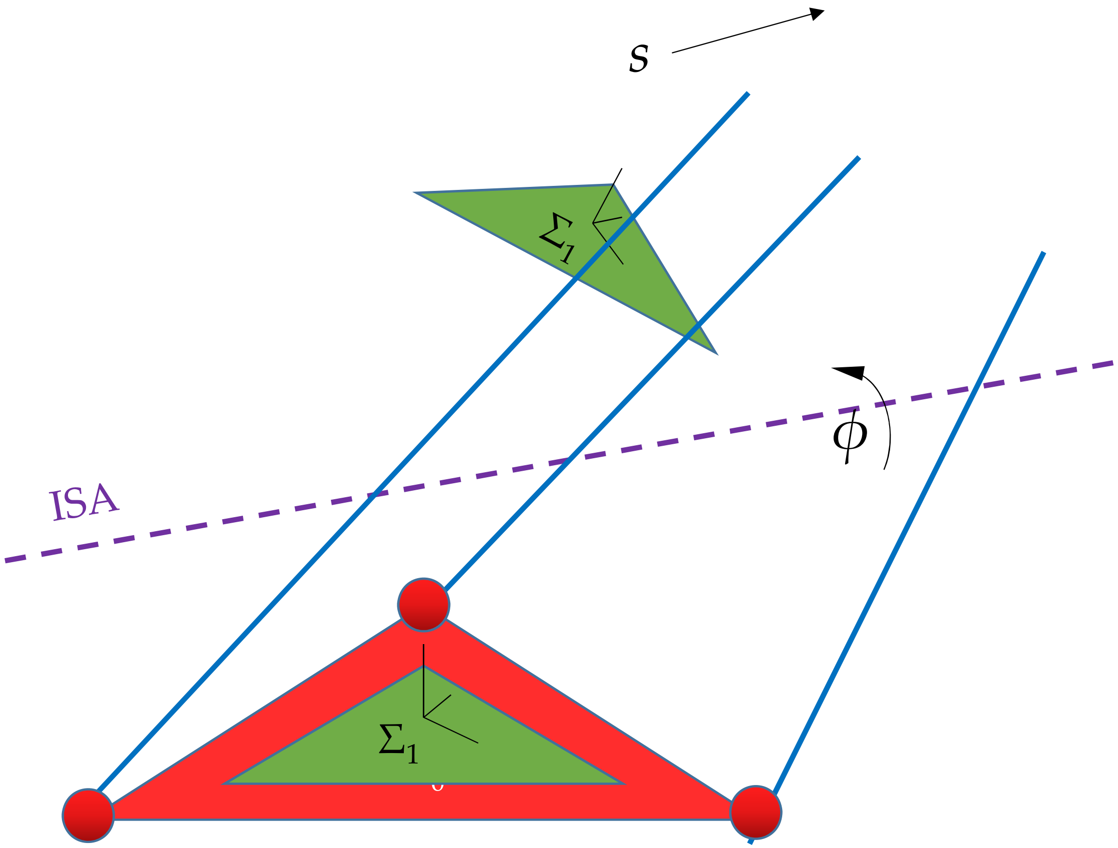

Instantaneous screw axis

Plücker-coordinates of the ISA

$$
\begin{aligned}
p_{01} &= (-x_1^2 - x_2^2 - x_3^2)x_1, & p_{23} &= x_0 y_0 x_1 - (-x_1^2 - x_2^2 - x_3^2)y_1 \\
p_{02} &= (-x_1^2 - x_2^2 - x_3^2)x_2, & p_{31} &= x_0 y_0 x_2 - (-x_1^2 - x_2^2 - x_3^2)y_2 \\
p_{03} &= (-x_1^2 - x_2^2 - x_3^2)x_3, & p_{12} &= x_0 y_0 x_3 - (-x_1^2 - x_2^2 - x_3^2)y_3
\end{aligned}
$$

$$p_{01}p_{23} + p_{02}p_{31} + p_{03}p_{12} = 0$$

Normalized Study-parameters

$$cos(\frac{\phi}{2}) = x_0 \quad ; \quad s = \frac{2y_0}{\sqrt{x_1^2 + x_2^2 + x_3^2}}$$

4 Singularities : 3-SPR parallel manipulator[1]

$$\mathrm{J}_i = \left(\frac{\partial g_j}{\partial x_k}, \frac{\partial g_j}{\partial y_k}\right) \text{ where } \quad i = 1,2\,; \quad j = 1, \ldots, 8\,; \quad k = 0, \ldots, 3$$

$$S_1 : x_3 \cdot p^7(x_1, x_2, x_3, y_0, y_1, y_2, y_3) = 0 \qquad \boxed{x_0 = 0}$$

$$S_2 : x_0 \cdot p^7(x_0, x_1, x_2, y_0, y_1, y_2, y_3) = 0 \qquad \boxed{x_3 = 0}$$

Constraint singularity

$$x_0 = x_3 = 0$$

other singularities

$$p^7(x_k, y_k) = 0,\ k = 0, 1, 2, 3$$

[1] Schadlbauer, J., Walter, D.R., and Husty, M.: A Complete Kinematic Analysis of the 3-RPS Parallel Manipulator, 15th National Conference on Machines and Mechanisms (2011).

4 Singularities : 3-SPR parallel manipulator

Other singularities in orientation workspace

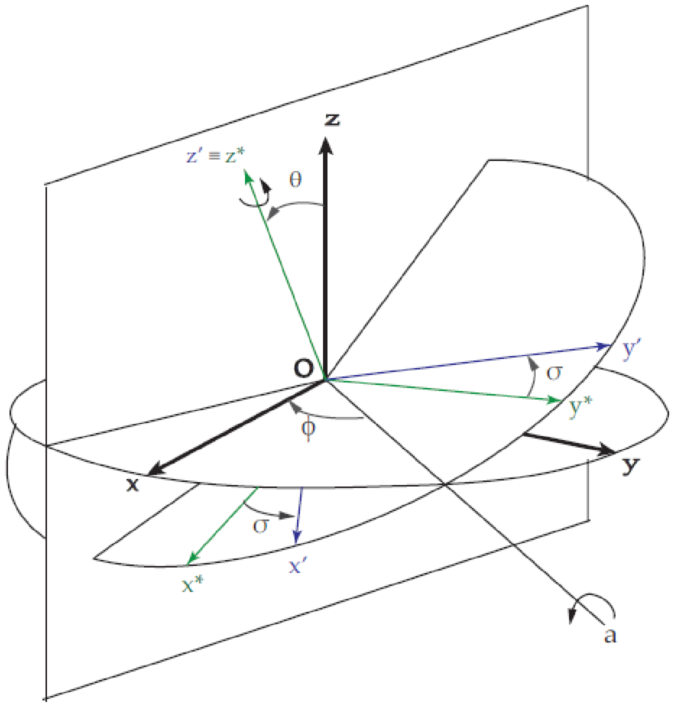

$$x_0 = \cos(\frac{\theta}{2})\cos(\frac{\sigma}{2})$$
$$x_1 = \sin(\frac{\theta}{2})\cos(\phi - \frac{\sigma}{2})$$
$$x_2 = \sin(\frac{\theta}{2})\sin(\phi - \frac{\sigma}{2})$$
$$x_3 = \cos(\frac{\theta}{2})\sin(\frac{\sigma}{2})$$

Tilt and torsion angles[5]

$$\mathbf{M}' = \begin{bmatrix} x_0^2+x_1^2+x_2^2+x_3^2 & 0 & 0 & 0 \\ X & {x_0}^2+{x_1}^2-{x_2}^2-{x_3}^2 & -2\,x_0x_3+2\,x_1x_2 & 2\,x_0x_2+2\,x_1x_3 \\ Y & 2\,x_0x_3+2\,x_1x_2 & {x_0}^2-{x_1}^2+{x_2}^2-{x_3}^2 & -2\,x_0x_1+2\,x_3x_2 \\ Z & -2\,x_0x_2+2\,x_1x_3 & 2\,x_0x_1+2\,x_3x_2 & {x_0}^2-{x_1}^2-{x_2}^2+{x_3}^2 \end{bmatrix}$$

Modified matrix of Study's kinematic mapping

[5] Bonev, I.A., Zlatanov, D., and Gosselin, C.M., ”Advantages of the modified Euler angles in the design and control of PKMs,” Parallel Kinematic Machines International Conference, Chemnitz, Germany, pp. 171-188, (2002).

4 Singularities : 3-RPS parallel manipulator

Singularities in each operation mode (in orientation workspace)

$x_0 = 0$: $\sigma = 180^0$

$h_1 = 1$
$h_2 = 2$

$x_3 = 0$: $\sigma = 0^0$

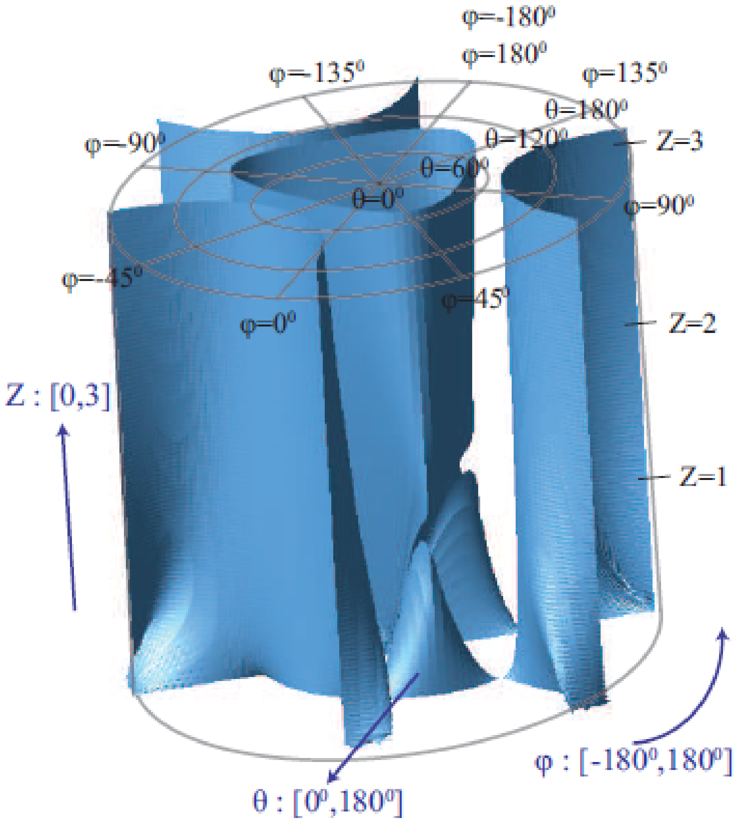

(a) Operation mode 1

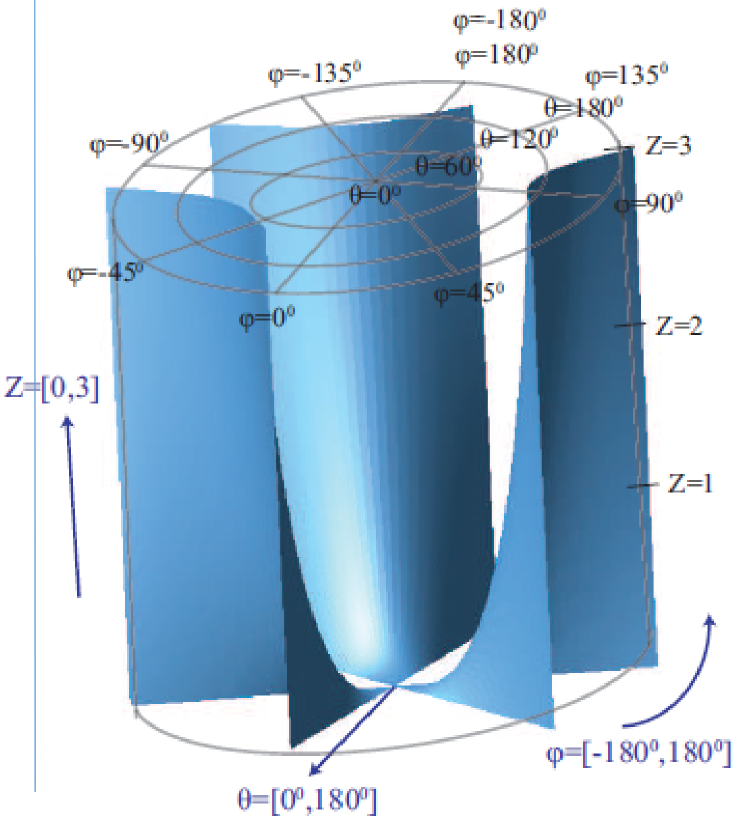

(b) Operation mode 2

4 Singularities : 3-SPR parallel manipulator

Singularities in each operation mode (in orientation workspace)

$x_0 = 0$: $\sigma = 180^0$

$h_1 = 1$
$h_2 = 2$

$x_3 = 0$: $\sigma = 0^0$

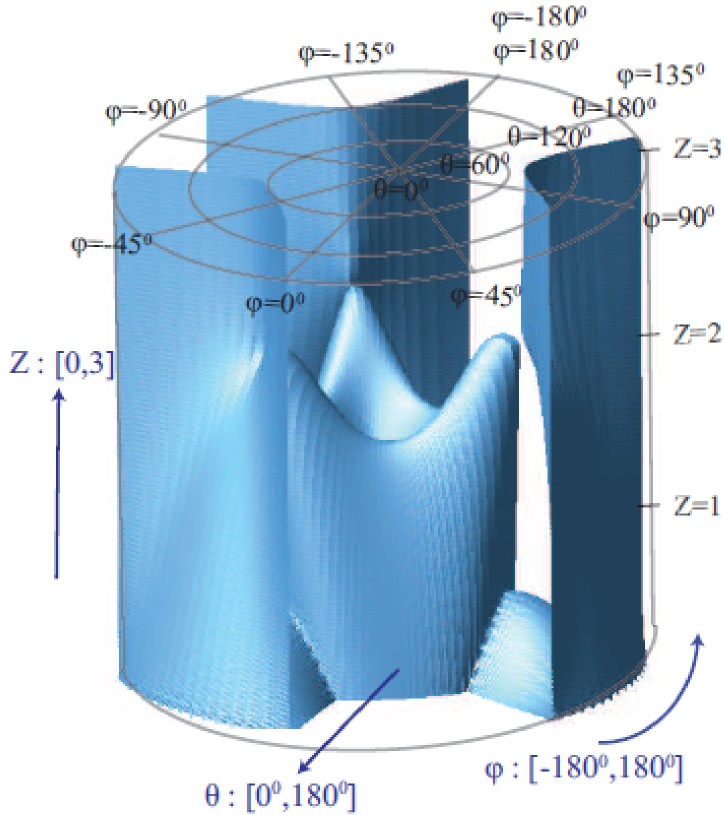

(a) Operation mode 1

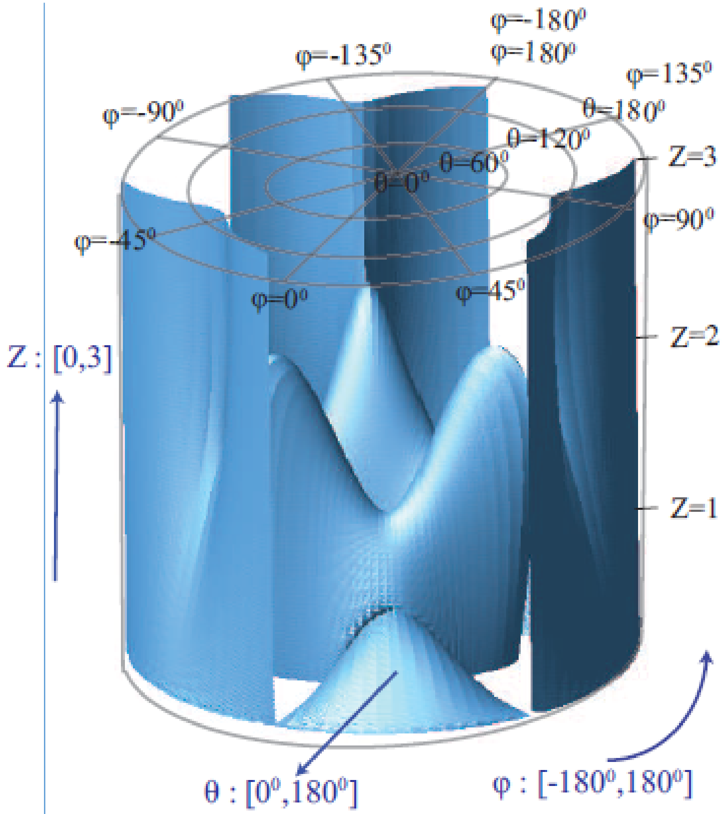

(b) Operation mode 2

4 Singularities : 3-SPR parallel manipulator

Singularities in each operation mode (in orientation workspace)

$x_0 = 0$: $\sigma = 180^0$

$h_1 = 1$
$h_2 = 2$

$x_3 = 0$: $\sigma = 0^0$

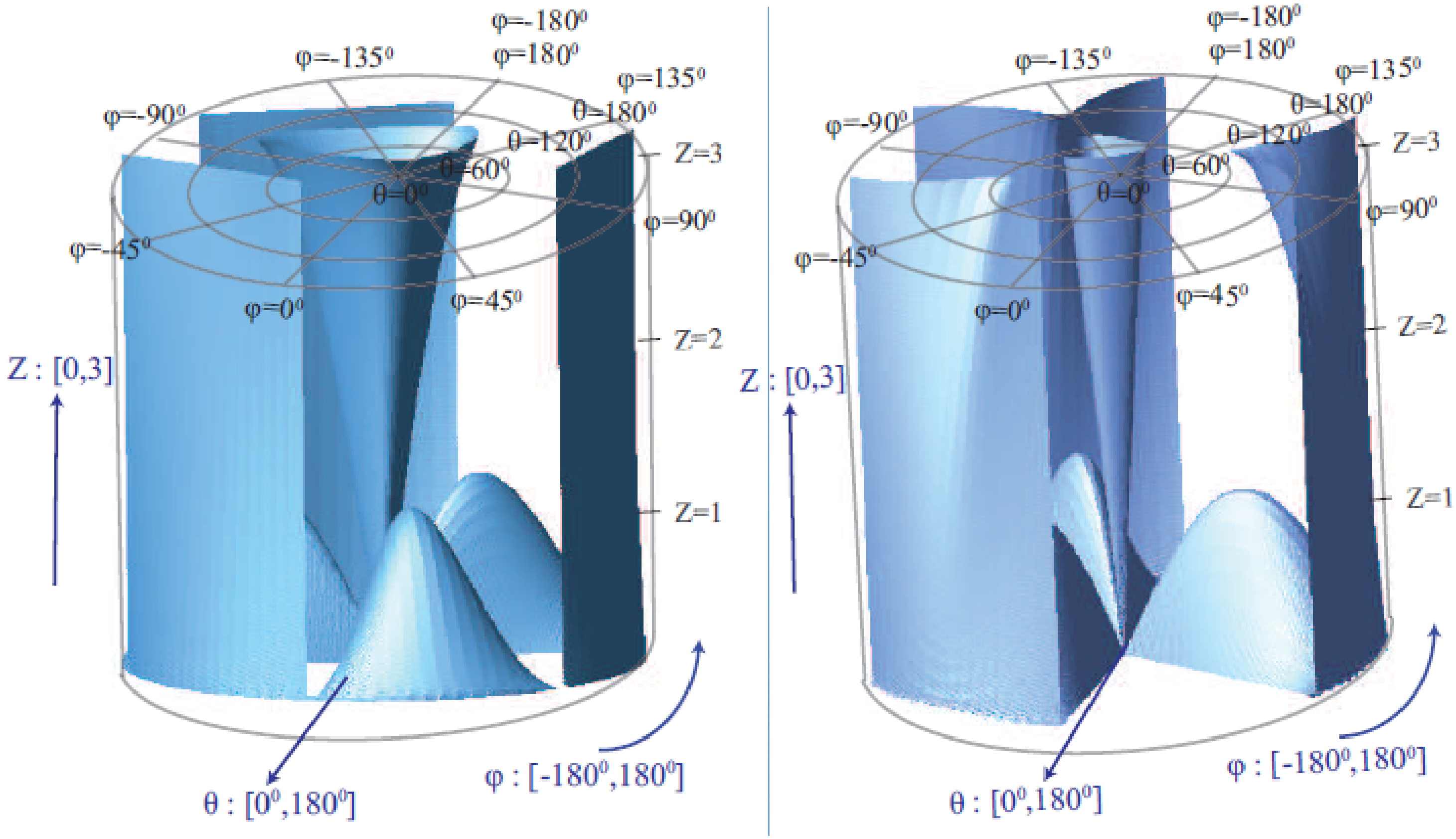

(a) Operation mode 1

(b) Operation mode 2

4 Singularities : 3-SP̲R parallel manipulator

Singularities in each operation mode (in orientation workspace)

$x_0 = 0$: σ = 180^0

$h_1 = 1$
$h_2 = 2$

$x_3 = 0$: σ = 0^0

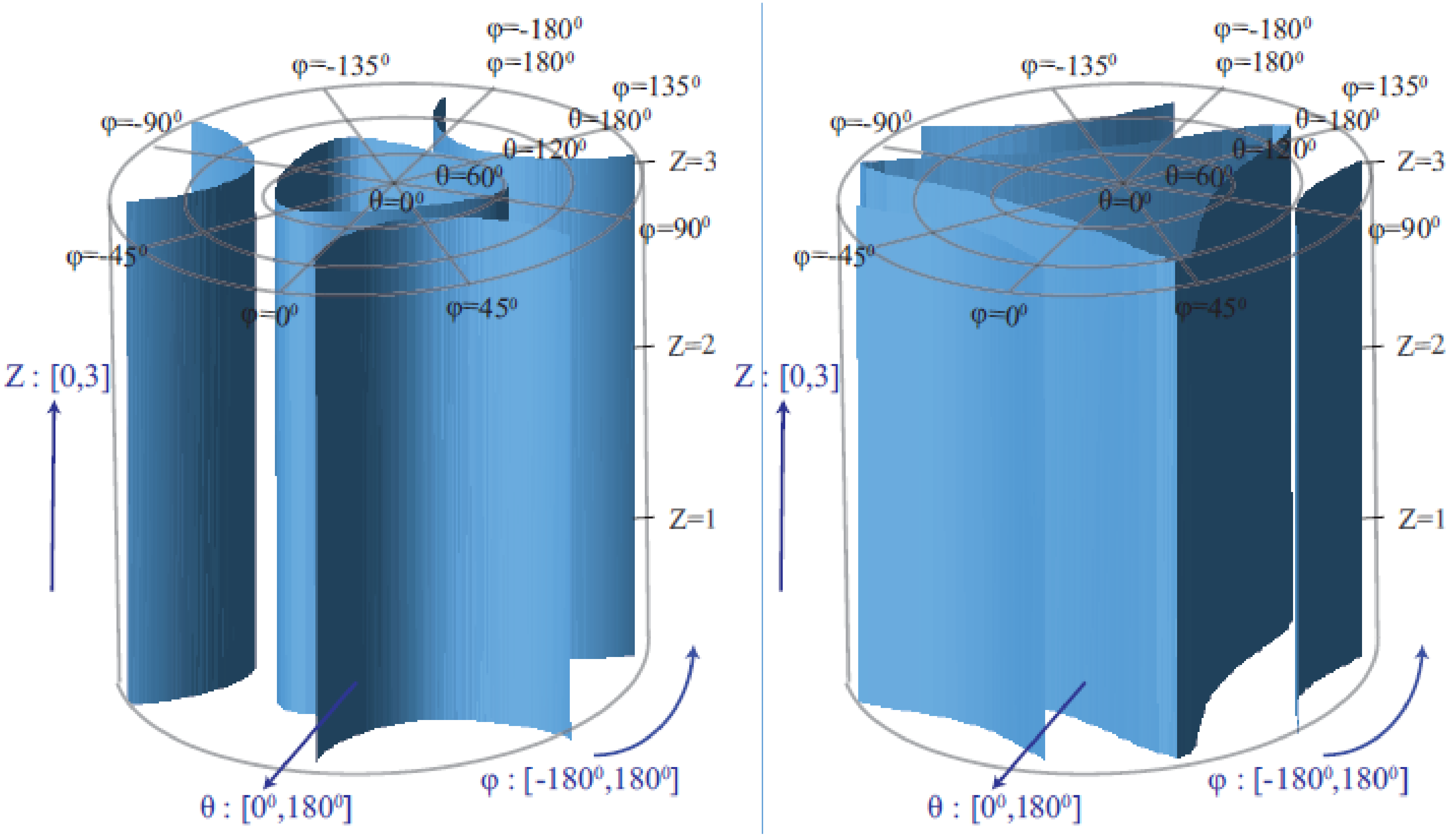

(a) Operation mode 1 (b) Operation mode 2

4 Singularities : 3-SPR parallel manipulator

Singularities in each operation mode (in orientation workspace)

Operation mode 1 :

$x_0 = 0$: $\sigma = 180^0$

$h_1 = 1$
$h_2 = 2$
$Z = 1$

Operation mode 2 :

$x_3 = 0$: $\sigma = 0^0$

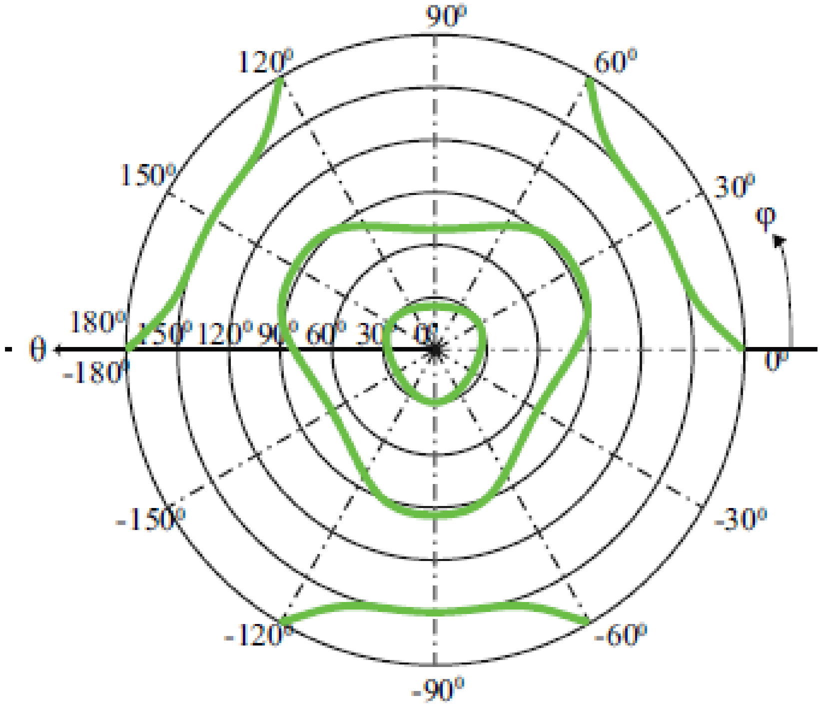

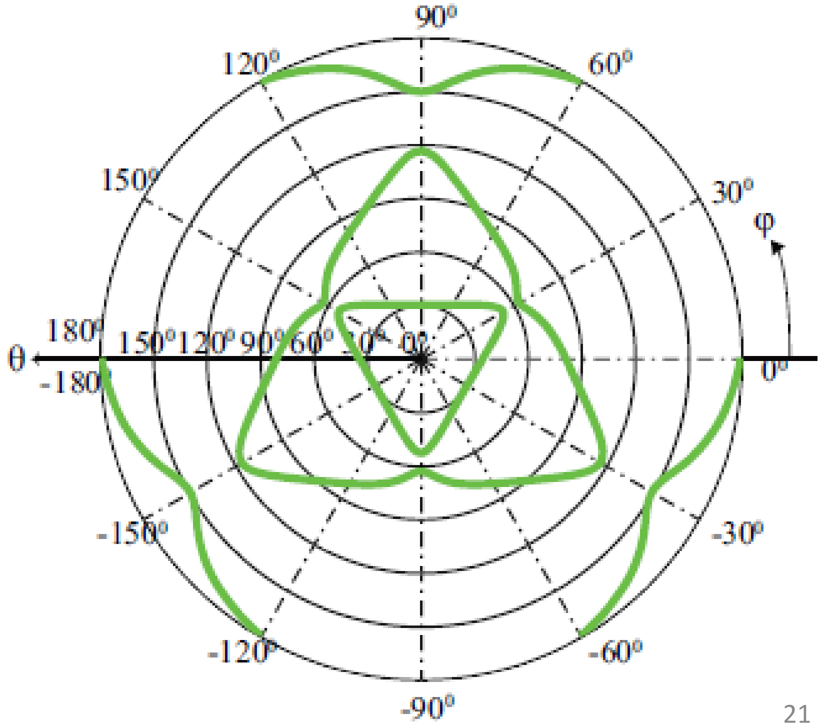

5 Maximum Inscribed Circle Radius[6]

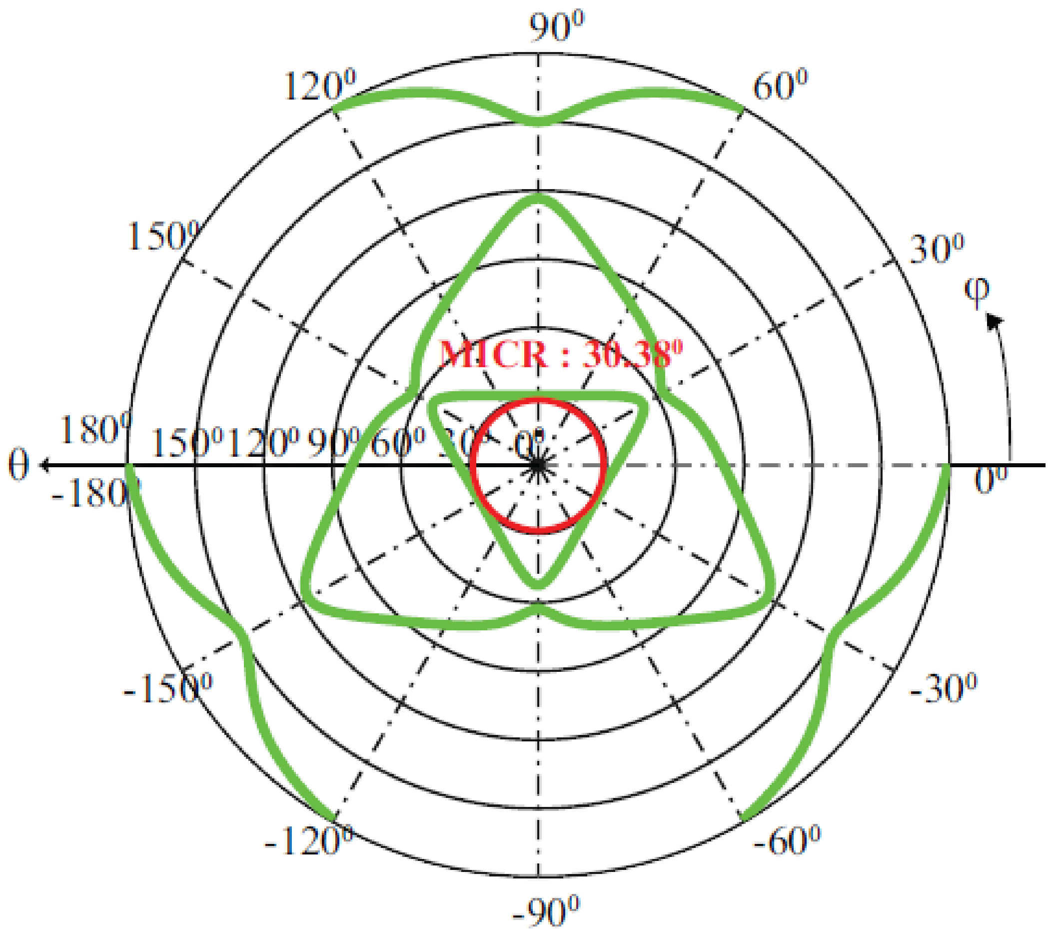

[6] Abhilash Nayak, Latifah Nurahmi, Philippe Wenger, Stéphane Caro, Comparison of 3-RPS and 3-SPR parallel manipulators based on their maximum inscribed singularity free circle, EUCOMES, Nantes, 2016

5 Maximum Inscribed Circle Radius

MICR vs. Z/h_1 for the 3-RPS PM

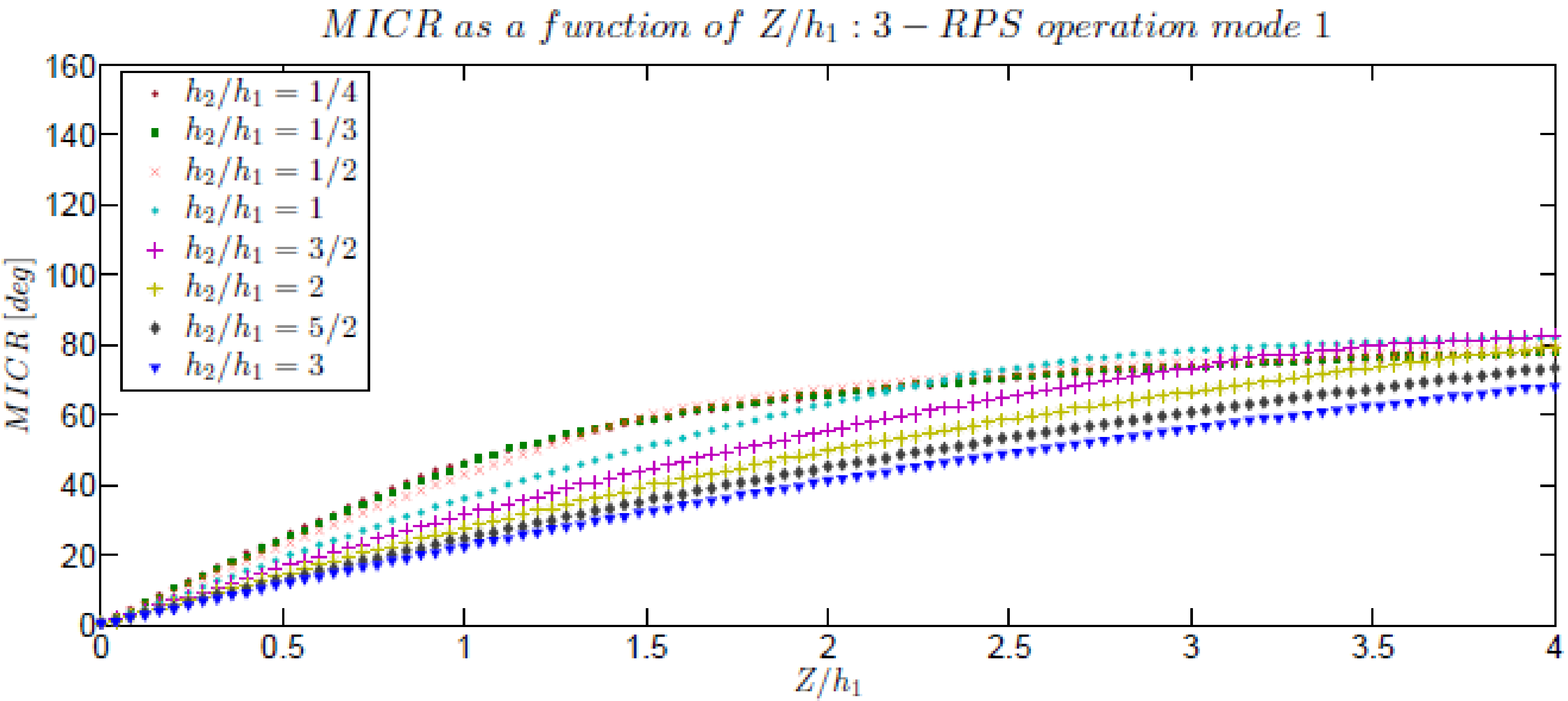

5 Maximum Inscribed Circle Radius

MICR vs. Z/h_1 for the 3-RPS PM

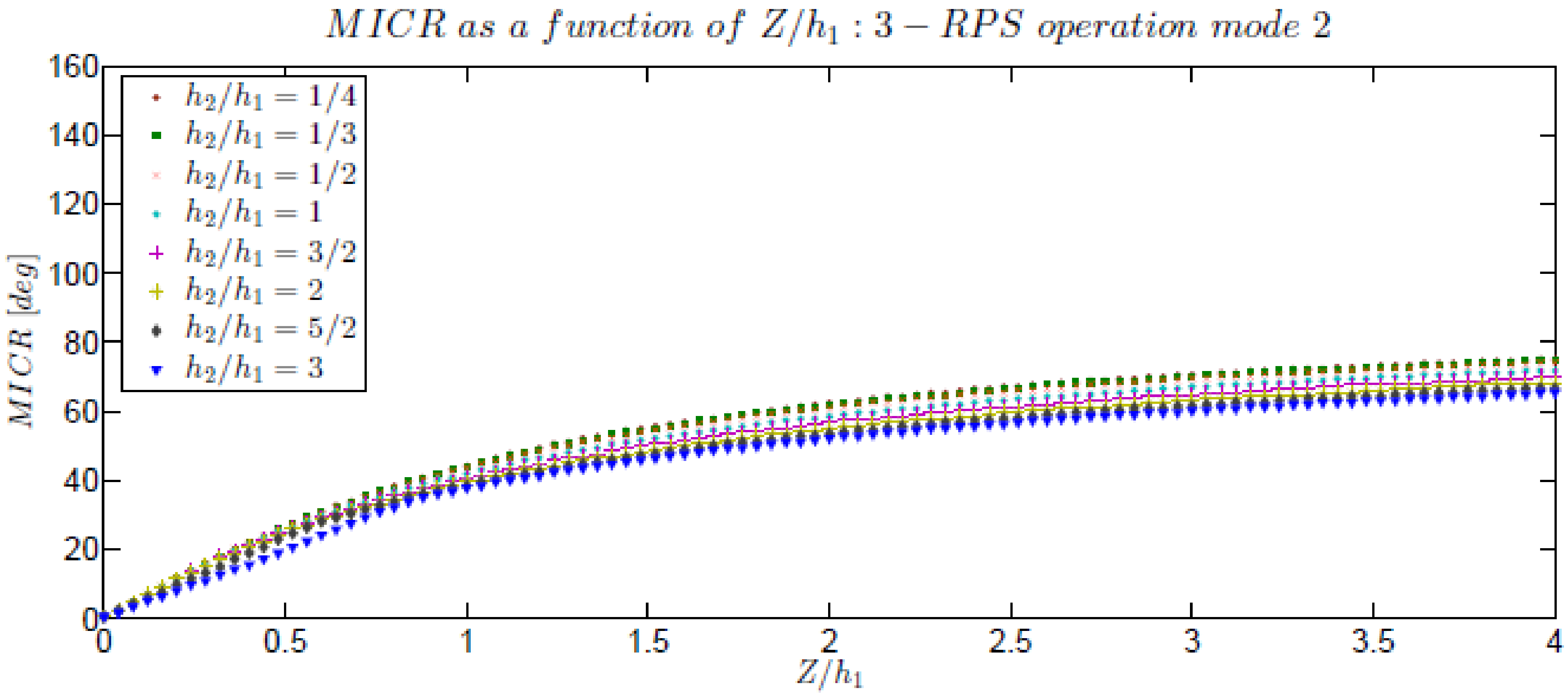

5 Maximum Inscribed Circle Radius

MICR vs. Z/h_1 for the 3-SPR PM

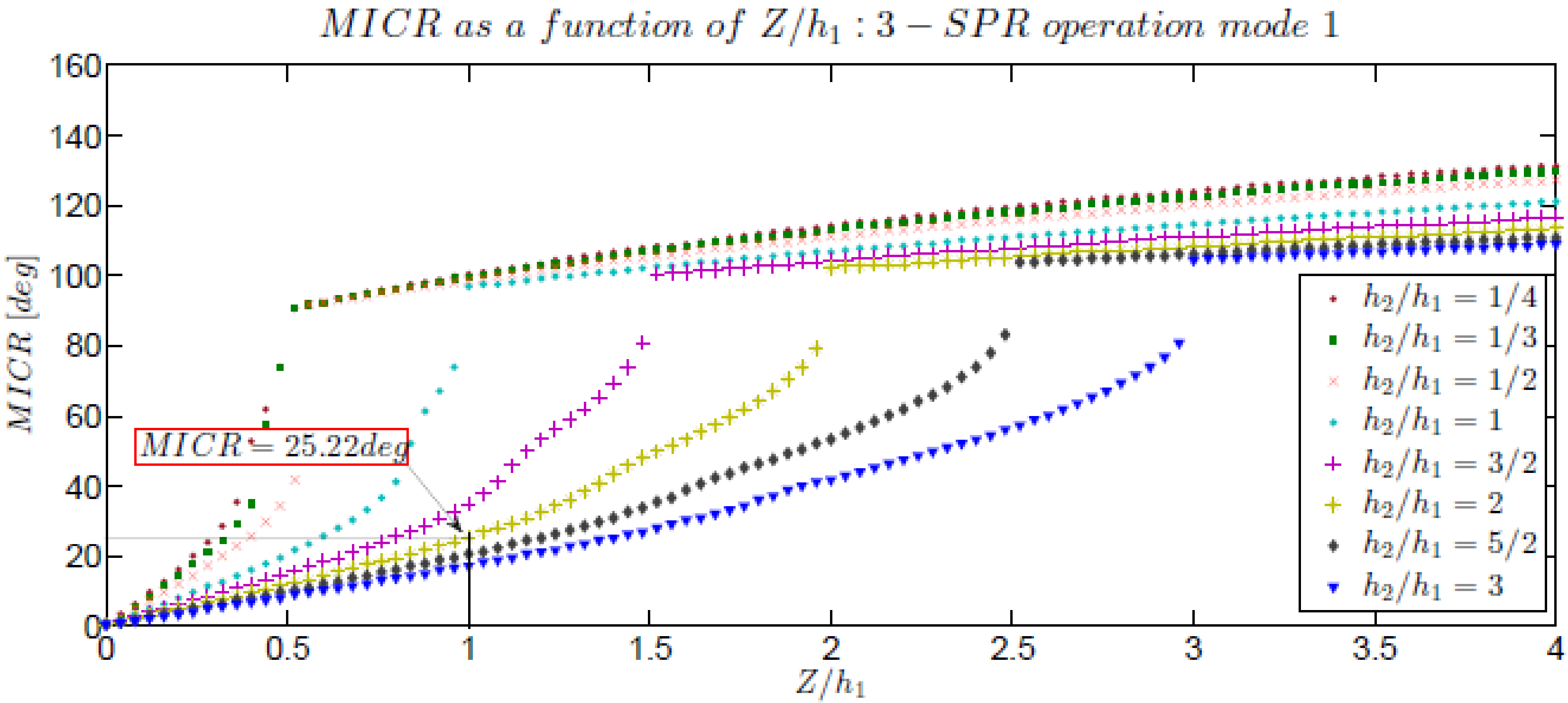

5 Maximum Inscribed Circle Radius

MICR vs. Z/h_1 for the 3-SPR PM

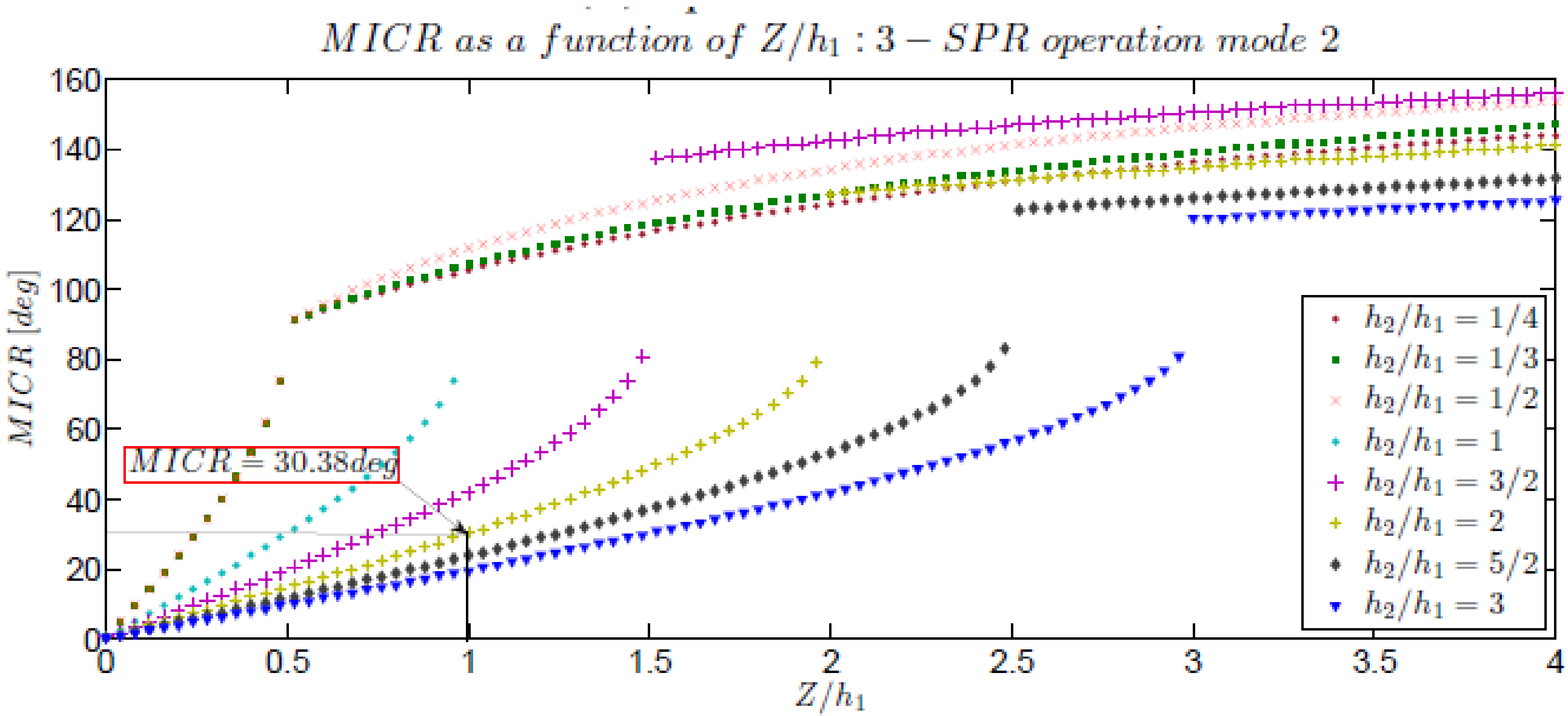

5 Maximum Inscribed Circle Radius

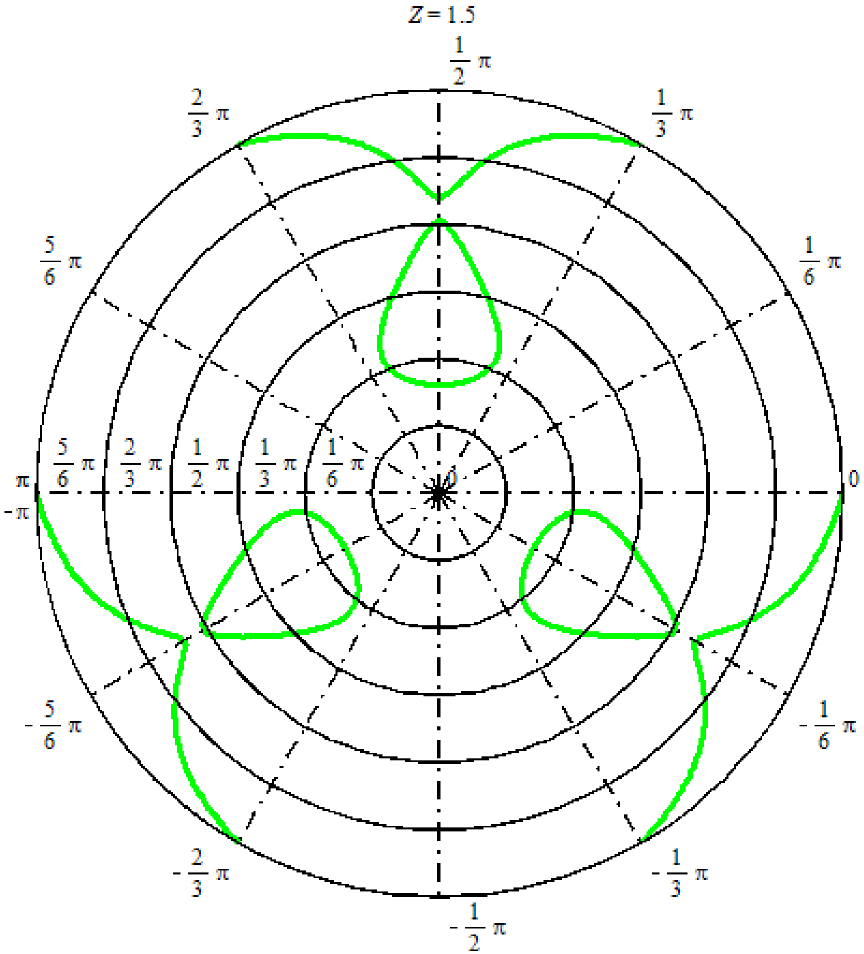

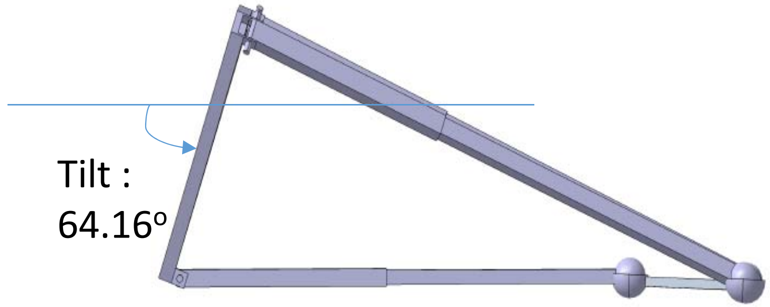

Operation mode 2 (x_3=0)

$h_2/h_1 = 2$
$Z/h_1 = 1.8$
Azimuth = 90°
Tilt = 64.16°

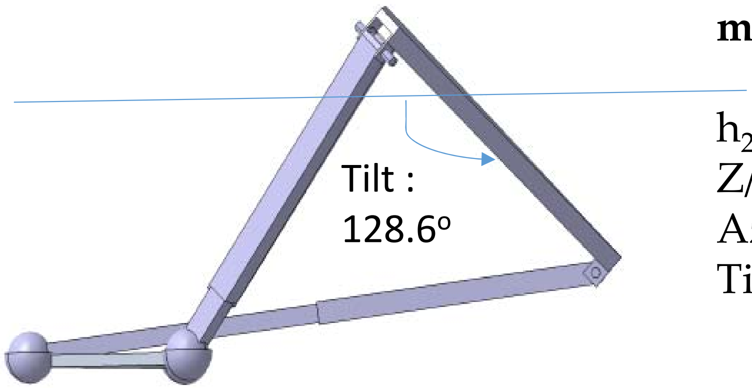

Operation mode 2 (x_3=0)

$h_2/h_1 = 2$
$Z/h_1 = 2.2$
Azimuth = 90°
Tilt = 128.6°

5 Maximum Inscribed Circle Radius

Void at 90^0 tilt

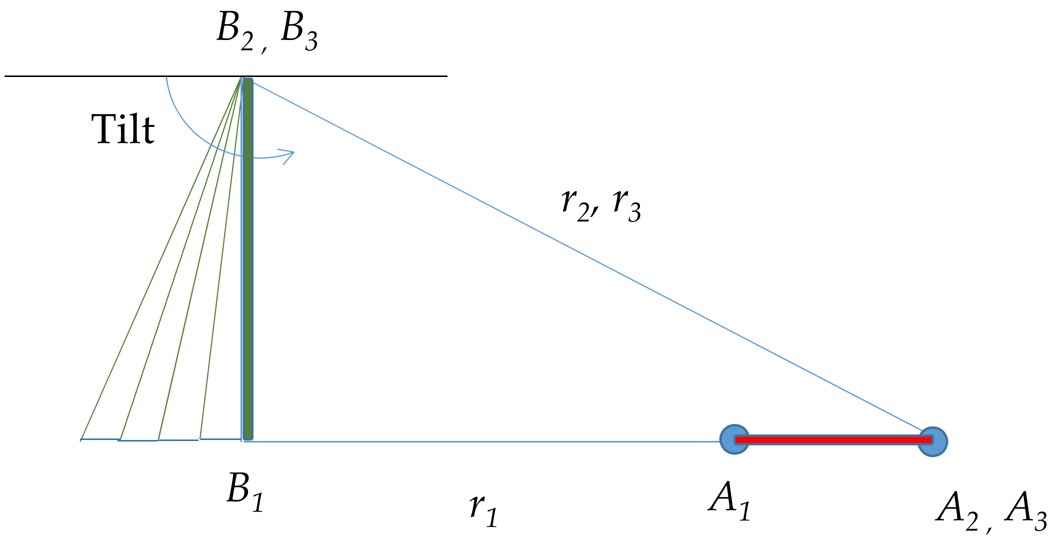

6 Parasitic motion

X and Y coordinates (operation mode 2, $x_3 = 0$)

3-S<u>P</u>R	$X := \frac{2Zx_0^3x_2 + 2Zx_0x_1^2x_2 + 2Zx_0x_2^3 - h_1x_0^2x_1^2 + h_1x_0^2x_2^2 + h_1x_1^4 - 6h_1x_1^2x_2^2 + h_1x_2^4}{(x_0^2 - x_1^2 - x_2^2)(x_0^2 + x_1^2 + x_2^2)}$ $Y := -\frac{2(Zx_0^3x_1 + Zx_0x_1^3 + Zx_0x_1x_2^2 - h_1x_0^2x_1x_2 - 2h_1x_1^3x_2 + 2h_1x_1x_2^3)}{(x_0^2 - x_1^2 - x_2^2)(x_0^2 + x_1^2 + x_2^2)}$	When, tilt=90^o and Z=h_2 $x_0^2+x_3^2-x_1^2-x_2^2 = 0$
3-R<u>P</u>S, 3-<u>P</u>RS, 3-<u>P</u>UU	$X = \frac{h_2(x_1^2 - x_2^2)}{x_0^2 + x_1^2 + x_2^2}$ $\quad$ $Y = -\frac{2h_2x_1x_2}{x_0^2 + x_1^2 + x_2^2}$	

6 Parasitic motion within MICR

3-S$\underline{P}$R (operation mode 2, $x_3 = 0$) : Z=1, $h_2 : h_1$ =2:1

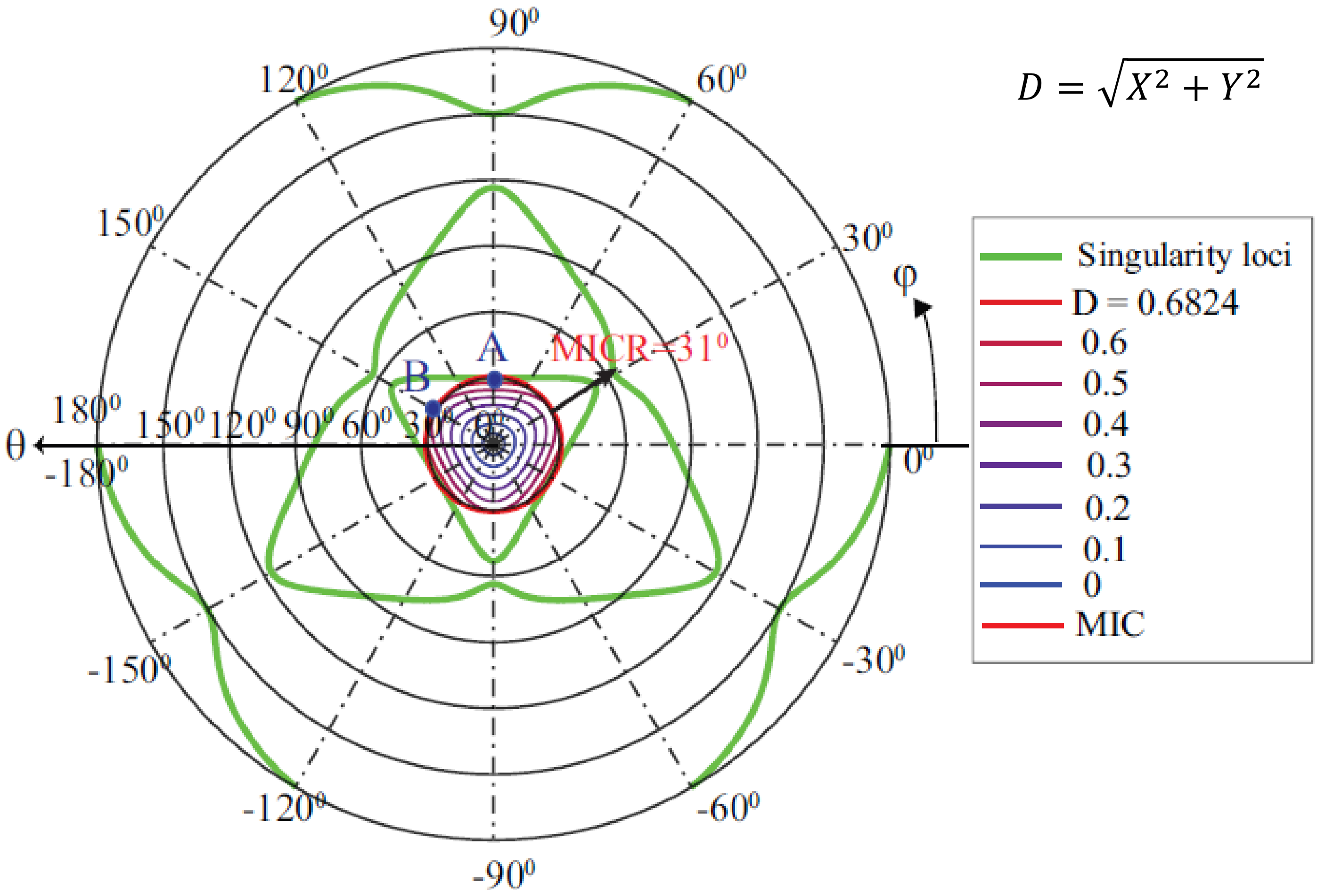

6 Parasitic motion within MICR

Maximum displacement vs. Z/h_1 for the 3-R$\underline{P}$S PM
Operation mode 1

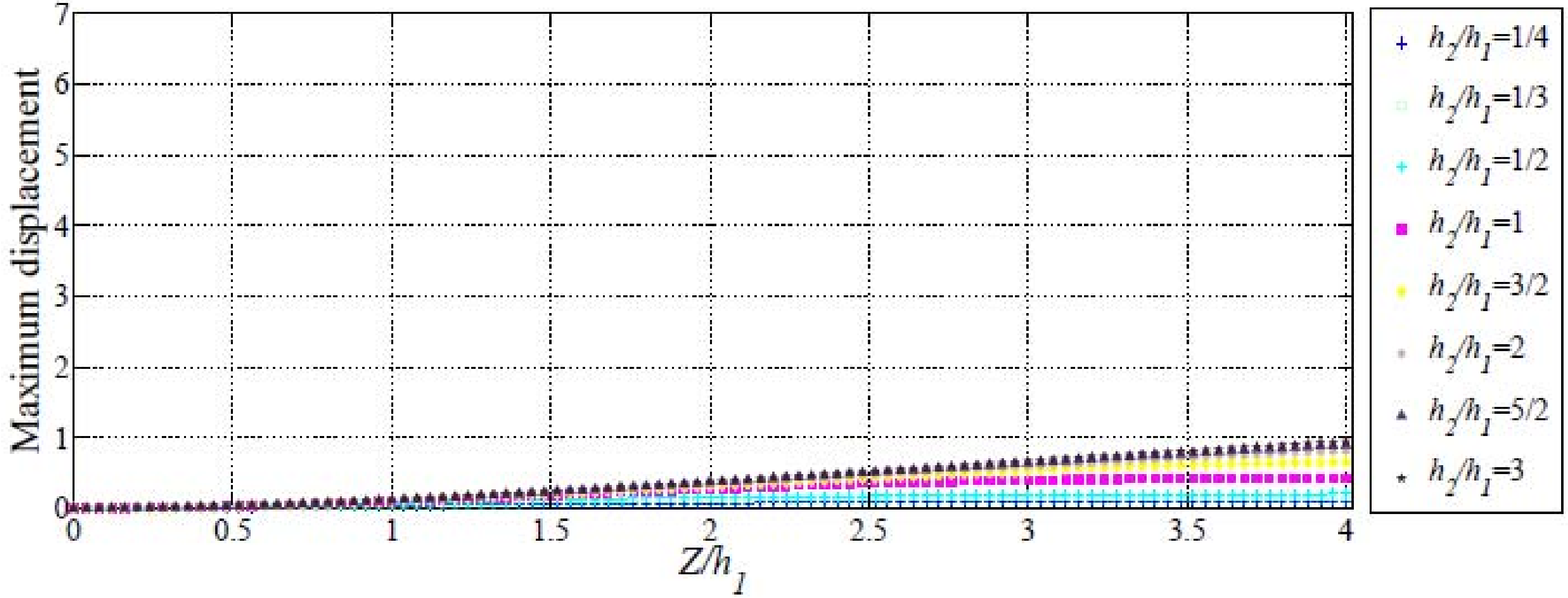

6 Parasitic motion within MICR

Maximum displacement vs. Z/h_1 for the 3-RPS PM
Operation mode 2

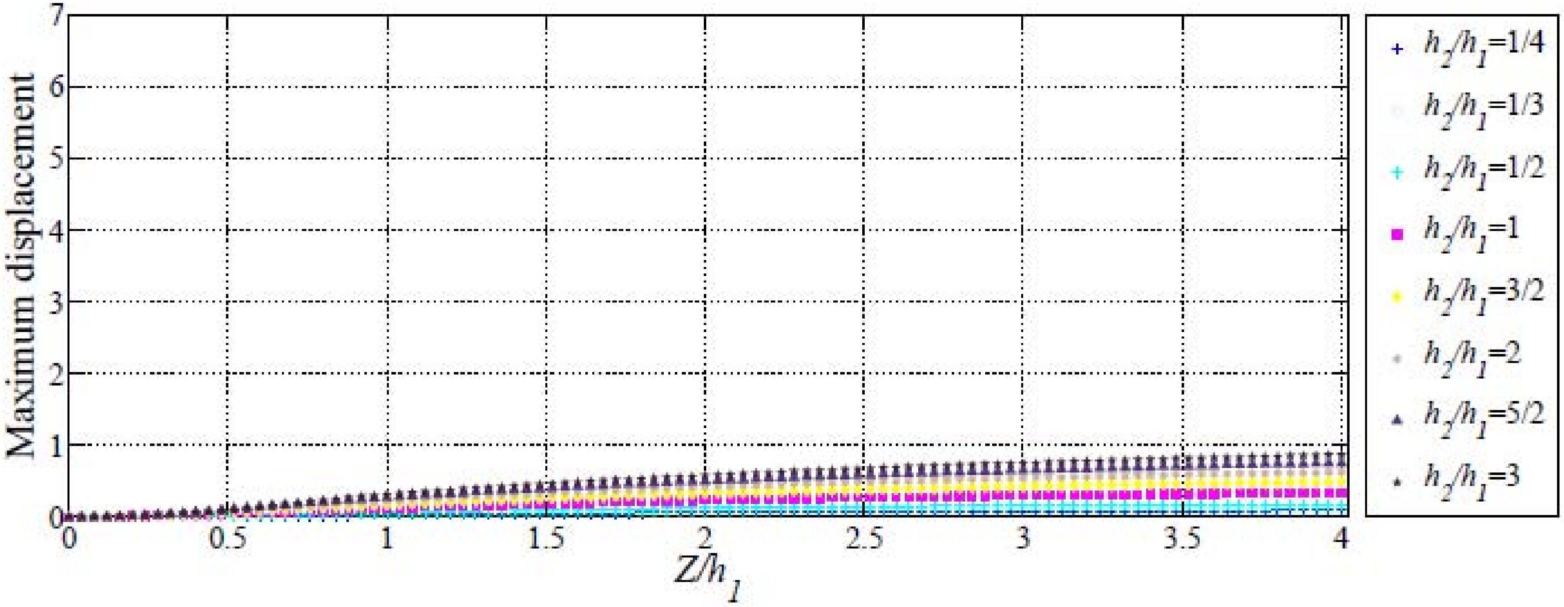

6 Parasitic motion within MICR

Maximum displacement vs. Z/h_1 for the 3-SPR PM
Operation mode 1

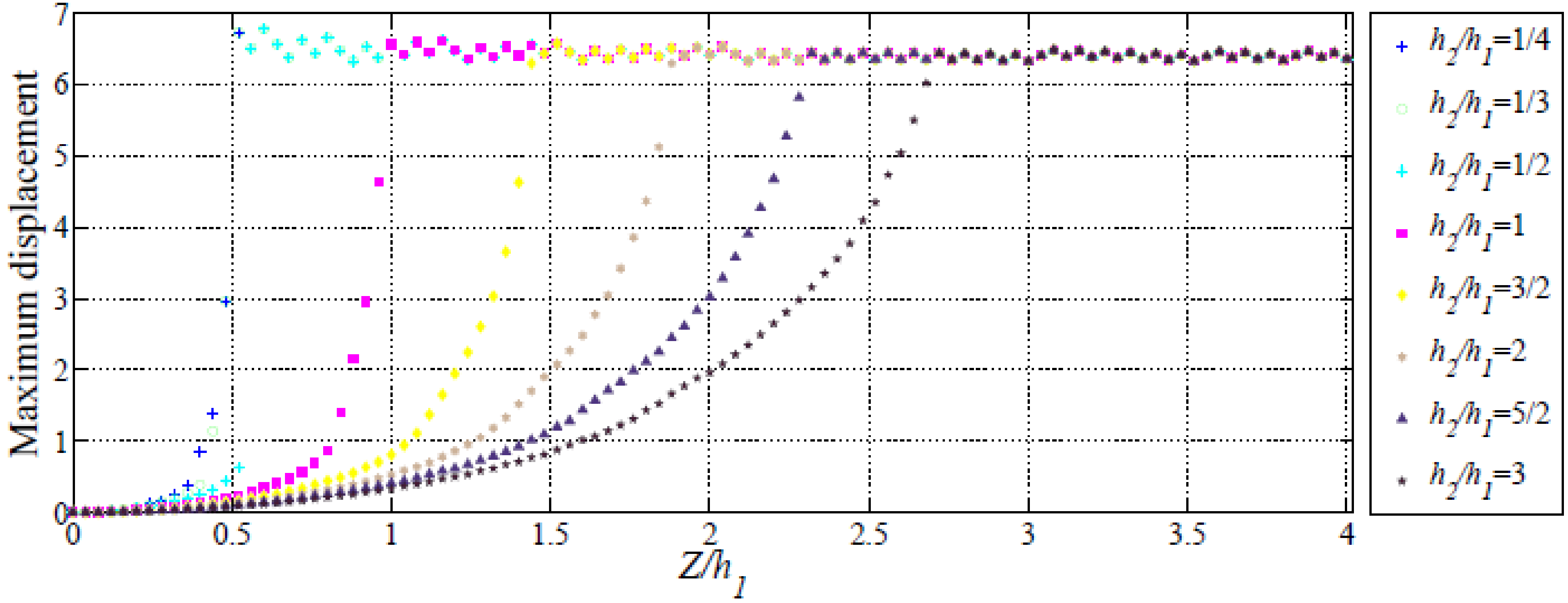

6 Parasitic motion within MICR

Maximum displacement vs. Z/h_1 for the 3-SPR PM
Operation mode 2

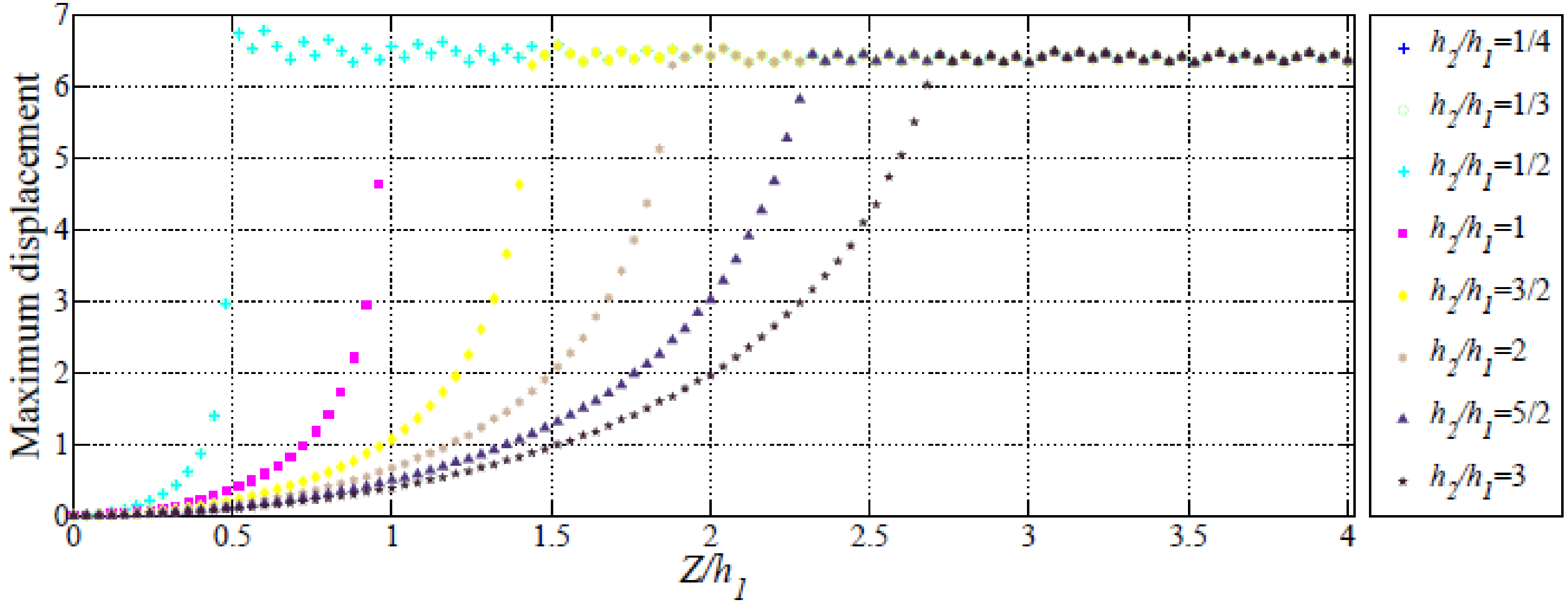

6 Conclusions and future work

- MICR and parasitic motion curves to compare zero-torsion PMs
- Larger singularity regions and higher parasitic motion for the 3-SPR PM.
- Discontinuity in MICR values for the 3-SPR PM : void in the orientation workspace.

- Comparing the zero-torsion PMs based on the type of motion.
- Considering all the existing zero-torsion manipulators (3-RPS, 3-SPR, 3-PRS, 3-RRS, 3-PPS, 3-RSR, 3-PSP, 3-PUU) ; Synthesis of zero-torsion PMs using screw theory or algebraic geometry tools.

Merci

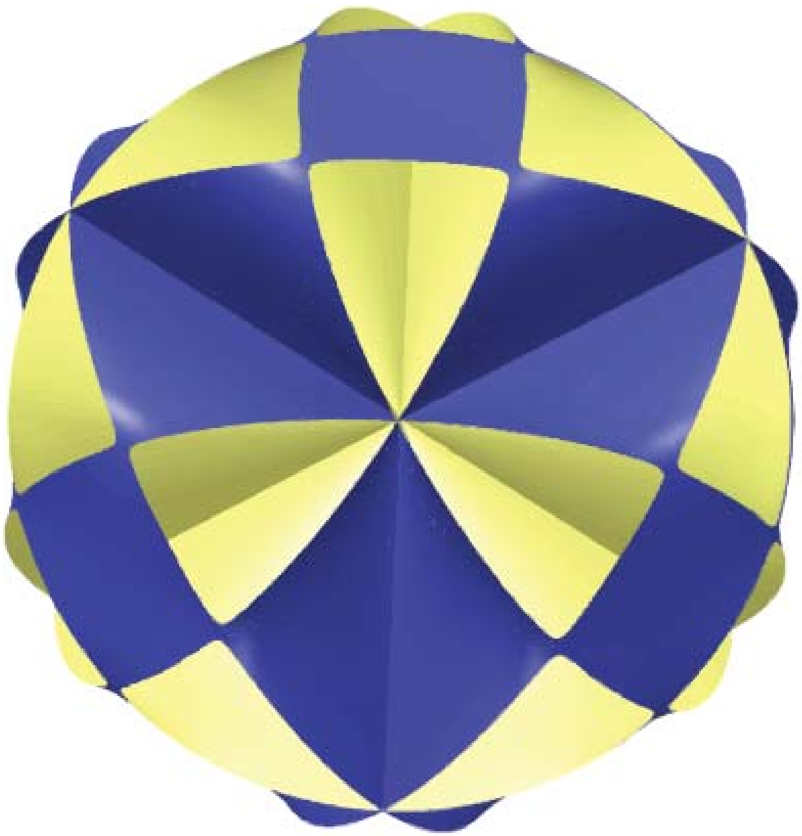

A cross-section view of singularity surface of the 3-RPS parallel manipulator in its joint space.